

Device Localization using mmWave Ranging with Sub-6-assisted Angle of Arrival Estimation

Nebojsa Maletic[†], Vladica Sark[†], Jesús Gutiérrez[†] and Eckhard Grass^{†‡}

[†]IHP, Im Technologiepark 25, 15236, Frankfurt (Oder), Germany

[‡]Humboldt-Universität zu Berlin, Germany

Email: {maletic, sark, teran, grass}@ihp-microelectronics.com

Abstract—Millimeter wave (mmWave) communication is a promising solution for achieving high data rates and low latency in future wireless networks. 5G systems are expected to fulfill these strict requirements using, among others, mmWaves. The nature of the communication in these bands considering human mobility make the challenges even complex for reasons like high beam training overhead. Features like ranging and localization are becoming key to overcome these limitations. In this paper, we address the problem of device localization in the mmWave band. We propose a solution that leverages the co-existence of Sub-6 GHz and mmWave connectivity at access and mobile nodes. Our solution relies on Angle of Arrival estimation using Sub-6 signal at the access node. This information is provided to the mmWave part for subsequent beam training phase and high-resolution ranging. To validate the proposed solution, a number of measurements are performed showing its feasibility.

I. INTRODUCTION

To meet high demands for high data-rates access, capacity of current wireless networks has to increase. There is an aim of $1000\times$ increase in data traffic predicted by 5G till 2020 [1], which might not be achieved with current 4G networks. That is why new spectrum bands in the millimeter wave (mmWave) spectrum (i.e. 30 – 300 GHz) are seen promising due to large amount of unutilized bandwidth available worldwide [2], [3], [4]. MmWave communication can provide gigabit-per-second (Gbps) data rates and low latency. Solutions are already available on the market for the 60 GHz band, like those for local and personal networks following IEEE 802.11ad [5] and IEEE 802.15.3c [6] standards, respectively. Currently, both academia and industry are investigating 60 GHz solutions for cellular fronthaul and backhaul networks [7]. However, the high data rates come at the cost that this communication needs to be highly directional. This is associated with the inherent path loss at mmWave frequencies [4]. Nevertheless, small wavelength (5 mm at 60 GHz) allows deployment of large antenna arrays which can be packed in small form factor. This way, mmWave systems can achieve sufficient beamforming gain to combat the inherent high free-space path loss and to provide sufficient link budget [3], [4]. In addition to Gbps data communication, there are other features like localization and ranging that can be beneficial to mmWave systems. For example, combined data communication and high-resolution ranging has been demonstrated in [8]. Regarding localization,

this feature can be useful for new services such as safety critical applications, augmented reality [9], assisted living [10]. In addition, position information can be used for beam training overhead reduction as well as handovers between access points.

Localization using mmWave signals is gaining more attention nowadays. In [11], [12], classical localization methods using different signal features like Received Signal Strength (RSS), Time of Arrival (ToA) and Time Difference of Arrival (TDoA) are investigated. A method for mmWave localization and tracking using RSS and signal phase called “mTrack” is proposed in [13]. In [14] a method for mmWave device localization in indoor environment is proposed. This method does not require any knowledge about the surrounding environment or the location and the number of access points. In [15] simultaneous localization and mapping (SLAM) has been investigated using mmWave signals. Different methods for localization using single anchor node exploiting multi-reflected paths are given in [16]. In [17] joint localization and position orientation for mmWave is investigated. Impact of beamforming strategies on mmWave localization is analyzed in [18]. Nevertheless, according to [9], [19] multi-connectivity i.e. a legacy network link and an mmWave link, shall be supported in future wireless networks. This means both access nodes and mobile nodes will have Sub-6 and mmWave interfaces. In such scenario, information from a lower frequency band can be used to support the communication in the mmWave band. In [20] the authors have investigated the use of channel state information acquired at the lower frequency band (Sub-6 GHz) to estimate the mmWave channel. Out-of-band measurements acquired in the Sub-6 band are used to reduce the beam training overhead for mmWave communication in [21] and [22].

Owing to the aforementioned, in this paper we envision a solution for mmWave localization exploiting multicommunicability - Sub-6 and mmWave - at access and mobile nodes. We use the Sub-6 band as a side channel to determine Angle of Arrival (AoA) at the side of access node. This information is provided to the mmWave part to speed up the beam training process, after which mmWave ranging is performed to obtain centimeter precision distance estimates. Using the estimated AoA and the distance estimate, a fairly accurate position of mobile node can be obtained. To prove this, AoA estimation, beam training and ranging measurements are performed showing the

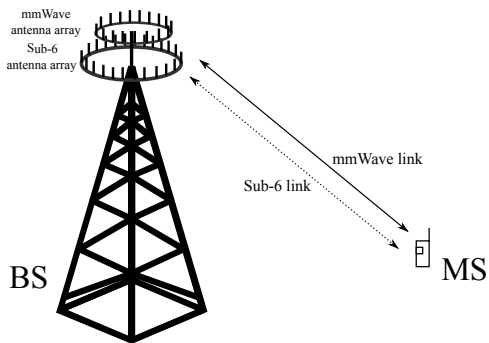


Fig. 1. System architecture example.

feasibility of the proposed solution.

The remainder of this paper is organized as follows: in Section II we introduce the concept and system architecture. Key signal processing blocks are described in Section III. Implementation and evaluation of the proposed solution is presented in Section IV, while concluding remarks and future work is given in Section V.

II. SYSTEM CONCEPT AND ARCHITECTURE

We consider a system with two endpoints both having Sub-6 and mmWave radios. At each endpoint the two radio interfaces are synchronized. In our scenario one endpoint is stationary - referred as base station (BS) - and the other endpoint is mobile - referred as mobile station (MS). The MS has a single Sub-6 antenna and mmWave antenna array, while the BS is equipped with antenna arrays in both frequency bands. Both endpoints have a single radio-frequency (RF) chain at 60 GHz and beamforming is performed in RF domain using a network of phase shifters. The system architecture is shown in Fig. 1.

The BS architecture is shown in Fig. 2. It consists of an mmWave device on top and a Sub-6 at the bottom. The mmWave part comprises a uniform linear array (ULA) of N_a antennas and a beamforming unit with beam steering capabilities with a certain angular range. Its Sub-6 counterpart has an antenna array of P omni-directional antennas and it is able to detect signal direction of any paired MS. The MS has an mmWave device with an ULA of M_a antennas and a Sub-6 device with a single antenna element. The MS transmits periodically beacon frames in the Sub-6 band to the BS. The BS acquires this signal with the antenna array and processes it to obtain an estimation of the AoA. The BS replies to the MS with a reply frame in the same band signaling the upcoming beam training phase. In addition this signal can carry additional information, e.g. beam training request from the BS side. The BS uses the estimated AoA using the Sub-6 transmission to steer the beam toward the MS in the mmWave band accordingly. The MS trains its beams and chooses the one with the highest signal-to-noise ratio (SNR). Once the beams are aligned, BS and MS perform distance estimation using Two-way ranging (TWR). Finally, having both AoA and distance estimation between BS and MS, the BS can determine the position of the MS with respect to its position.

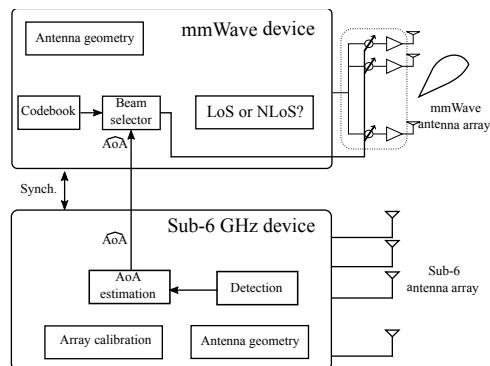


Fig. 2. BS multi-band node architecture.

III. SIGNAL PROCESSING ENGINE

Once the general procedure has been described, we present key signal processing steps to obtain position estimate: AoA estimation, beam training and ranging.

A. Angle of arrival estimation

The BS is equipped with an antenna array of P omni-antennas in the Sub-6 band and is able to estimate the angle of arrival (AoA) of the incoming signal from the MS. For this, different methods can be used, from which the most known methods are MUSIC [23], root-MUSIC [24] and ESPRIT [25]. In this work, our focus is on MUSIC-based methods.

The theory behind AoA estimation using MUSIC-based methods is as follows. An ULA consists of P isotropic antennas separated from each other with a distance of $d \leq \lambda/2$, where λ is the wavelength of the plane wave received by the array. We consider L narrowband plane waves impinging on the ULA from directions $\theta_1, \theta_2, \dots, \theta_L$ from the main response axis. We assume $\pi/2 \leq \theta_1 \leq \theta_2 \leq \dots \leq \theta_L \leq -\pi/2$. At the time instant k , the received signal vector $\mathbf{x}(k) \in \mathbb{C}^{P \times 1}$ can be expressed as

$$\mathbf{x}(k) = \sum_i \mathbf{a}(\theta_i) s_i(k) + \mathbf{n}(k), \quad (1)$$

where $s_i(k)$ is the complex envelope of the i -th signal, $\mathbf{n}(k) \in \mathbb{C}^{P \times 1}$ is the noise vector at the time instant k , and $\mathbf{a}(\theta_i)$ is the array response vector defined as [26]

$$\mathbf{a}(\theta) = \frac{1}{\sqrt{P}} \left[e^{j \frac{2\pi}{\lambda} d \sin(\theta)}, \dots, e^{j(P-1) \frac{2\pi}{\lambda} d \sin(\theta)} \right]^T. \quad (2)$$

The expression in (1) can be written in matrix form as

$$\mathbf{x}(k) = \mathbf{A}\mathbf{s}(k) + \mathbf{n}(k), \quad (3)$$

where $\mathbf{A} = [\mathbf{a}(\theta_1), \mathbf{a}(\theta_2), \dots, \mathbf{a}(\theta_L)] \in \mathbb{C}^{P \times L}$ and $\mathbf{s}(k) = [s_1(k), s_2(k), \dots, s_L(k)]^T \in \mathbb{C}^{L \times 1}$. MUSIC-based algorithms estimate AoA based on the covariance matrix of the received signal, which is given by

$$\mathbf{R} = \mathbb{E} [\mathbf{x}(k)\mathbf{x}(k)^H] = \mathbf{A}\mathbf{S}\mathbf{A}^H + \sigma^2\mathbf{I}_P, \quad (4)$$

where \mathbf{S} is the transmitted data covariance matrix given as $\mathbb{E} [s(k)s(k)^H]$ and \mathbf{I}_P is the identity matrix of size $P \times P$.

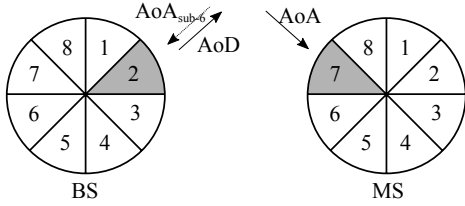


Fig. 3. mmWave beams (sectors) at BS and MS. Estimated Sub-6 AoA in sector 2, BS angle of departure (AoD) in sector 2 too, and MS AoA in sector 7.

Taking K snapshots of the received signal, a sample covariance matrix $\bar{\mathbf{R}} \in \mathbb{C}^{P \times P}$ can be calculated as

$$\bar{\mathbf{R}} = \frac{1}{N} \sum_{k=1}^K \mathbf{x}(k)\mathbf{x}(k)^H. \quad (5)$$

From the eigenvalues of $\bar{\mathbf{R}}$, both signal and noise powers can be obtained. There exist P eigenvalues, arranged in ascending order, from which the first ML eigenvalues correspond to noise subspace and the remaining L eigenvalues corresponds to signal subspace. Eigenvectors associated with the first ML eigenvalues form the noise subspace $\mathbf{U}_n \in \mathbb{C}^{P \times P-L}$. For the MUSIC method, pseudo-spectrum is calculated as $P(\theta) = 1/\mathbf{a}(\theta)^H \mathbf{U}_n \mathbf{U}_n^H \mathbf{a}(\theta)$. For the root-MUSIC method, the roots of the equation $\mathbf{a}(z^{-1})^H \mathbf{U}_n \mathbf{U}_n^H \mathbf{a}(z) = 0$ are used to obtain the estimates of DoAs, where $\mathbf{a}(z)$ is the array response vector with the argument z given by $z = e^{j \frac{2\pi}{\lambda} d \sin(\theta)}$.

B. Sub-6 GHz assisted beam training

We assume each endpoint (BS or MS) has a codebook consisting of N (M) beams or sectors, $N \geq N_a$ ($M \geq M_a$), to cover the angular space of interest. The estimated Sub-6 AoA is used to narrow down the angular search space. As a result, the number of BS mmWave beams used for beam training can be significantly reduced. The BS starts the beam training phase using the beam closest to the estimated AoA. In addition, it can request a beam training from the MS in order to refine its beam. This information can be provided within a acknowledge frame sent to the MS after AoA estimation. An example of BS and MS mmWave beams (sectors) and Sub-6 AoA is shown in Fig. 3.

We assume that two nodes are synchronized during Sub-6 communication. Once the Sub-6 AoA is available, the BS triggers the mmWave communication by sending a training frame to the MS towards the direction of the estimated AoA (see Fig. 3 - left). The training frame is sent M times in M successive time slots of duration T_s . At the same time, the MS is listening using different beams in each time slot to find its AoA. Based on the received SNR or other representative metric, the MS finds its best beam (Fig. 3 - right). If there is no beam training request from the BS side, the MS sends a reply frame to finalize the beam training session. If the reply frame is received at the BS, the beam training phase is finalized and the ranging phase can start. However, if the BS has requested beam refinement, after a reply frame is received, the beam

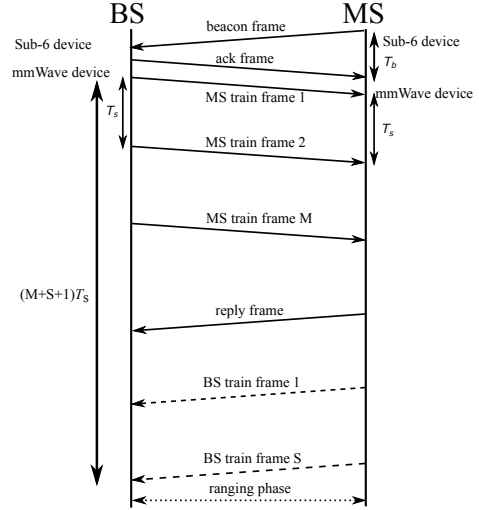


Fig. 4. System architecture example.

refinement phase at the BS starts. The BS trains its beam in successive ST_s time slots ($S < N$), while the MS sends to the BS the training frame using the previously trained beam. After ST_s time slots, the beam training phase ends. In the best case, when there is no beam refinement request from the BS, beam training procedure lasts for $M + 1$ time slots. With the BS beam refinement, it lasts for $M + S + 1$ time slots. The beam training procedure is shown in Fig. 4. Assuming $N = M = 16$, in the best case scenario Sub-6 GHz assisted beam training lasts for 17 time slots compared to exhaustive beam search which needs $N \cdot M + 1 = 257$ time slots. This way beam training latency can be reduced up to 93.4 %.

C. Ranging phase

A few different methods exist for distance and position estimation of a wireless node, based on the time-of-flight (ToF) estimation. The simplest one is based on ToA with the working principle shown in Fig. 5a. Both nodes must be synchronized before the ToA method is performed. Node N_1 transmits a waveform which is received by node N_2 . Node N_2 knows the exact time of transmission of the waveform and estimates the ToA of the received waveform. Having both time of transmission and the ToA, the ToF can be easily estimated. This method requires precise synchronization, which cannot be easily achieved. Two way ranging (TWR) is a ranging method which has significantly reduced synchronization requirements compared to ToA-based ranging. A basic TWR scheme is shown in Fig. 5b. The TWR starts from node N_1 , by transmitting a waveform to node N_2 . Node N_2 receives this waveform and replies back to N_1 with a similar waveform. Node N_1 measures the round trip time and node N_2 has a fixed reply time (or estimates it). The ToF can be easily estimated from the round trip time and the reply time.

IV. IMPLEMENTATION AND EVALUATION

This section presents the results of the evaluation of the system introduced in previous sections. For Sub-6 AoA estimation

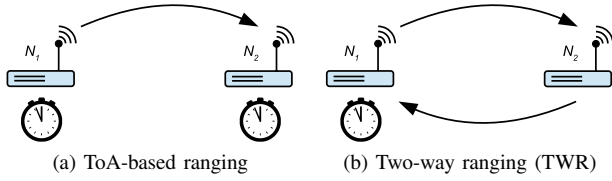


Fig. 5. ToF ranging methods.

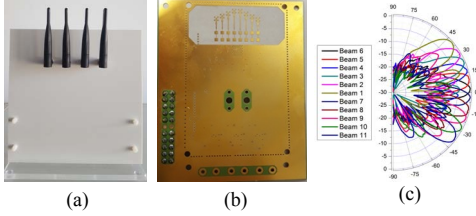


Fig. 6. Analog front-ends (AFEs): a) Sub-6 GHz dipole antenna array, b) 60 GHz antenna array, and c) beams associated with the 60 GHz antenna array.

experiments, software defined radio (SDR) devices USRPs X300/X310 from Ettus are used. The SDR MS is equipped with UBX160 daughterboard and has single dipole antenna, whilst the SDR acting as the BS has TwinRXs daughterboards connected to 4-dipole antenna array, as shown in Fig. 6 a). Omnidirectional dual band antennas (2.45 and 5.8 GHz) having 2.5 and 4.6 dBi gain, respectively, are used. For beam alignment and ranging tests, 60 GHz analog frontends (AFEs) with beamforming capability are used. The mmWave AFE consists of an up/down converter, a beamformer and a phased antenna array. The beamformer is an 8-channel bidirectional 60 GHz IC fabricated in IHPs SiGe:C 130nm BiCMOS technology [27]. The phased antenna array is an 8-element linear array with maximum gain of around 11 dBi at 61.5 GHz [28]. The antenna array AFE module with the beamformer and the associated beams in the range $-45^\circ - 45^\circ$ are shown in Figs. 6 b) and c). To generate the baseband signal at the BS side, an arbitrary waveform generator (AWG) is used. At the MS side, the baseband signal from the AFE is sampled using a digital sampling oscilloscope. The acquired samples are stored in memory and processed offline. Measurements are performed in an anechoic chamber of size 7 m (L) \times 4 m (W) \times 2.5 m (H) and an office environment.

A. Anechoic chamber measurement

The measurement setup is shown in Fig. 8a. The distance between the transmitter (MS) and the receiver (BS) is five meters. The system is calibrated according to [29]. The pilot tone is sent at the center frequency of 2.45 GHz with the sampling rate of 1 MSps. The test is performed for different angles. At the BS side, the signal is recorded and processed with MUSIC and root-MUSIC methods as described in Section III. Results are plotted in Fig. 7, whereas the estimated angles are given in Table I. Values that are obtained based on 1000 measurements shows that the estimated AoAs are within 2 degrees from the true AoA and that the standard deviation is below 0.2 degrees.

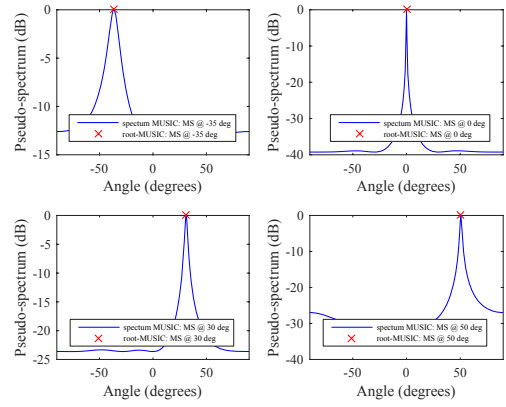


Fig. 7. AoA estimation of the pilot tone impinging the antenna array at the angles -35, 0, 30 and 50 degrees.

TABLE I
ANECHOIC CHAMBER: TRUE AND ESTIMATED AO A

AoA ($^\circ$)	-35	0	30	50
$\widehat{\text{AoA}}$ ($^\circ$)	-36.4	0.02	31.1	50.6

Next, the mmWave beam alignment experiment is performed. The transmitter (BS) and the receiver (MS) are positioned face to face at the distance of five meters. The signal frame used for this test consists of an IEEE 802.11ad single carrier preamble, a channel estimation field and a small data field. The signal is passed through a squared root-raised cosine (SRRC) filter with a roll-off factor of 0.25 spanned over 8 samples with oversampling factor 4 and sampled with the sampling frequency of 4 GSps. For each RX beam the frame was sent 10 times from TX using fixed beam and SNR is estimated. The estimated SNR values for beams 2, 4, 5, 6, 7, 8, and 10 are given in Table II. Using the maximal measured SNR policy, Rx finds the best beam for subsequent communication and ranging (in this case beam 6).

For the mmWave ranging measurement, a ToA approach is used as TWR cannot be implemented using the given setup. Nevertheless, it can be assumed the variance of the distance estimate using TWR approach results in twice the variance using ToA. This is true if the estimates follow normal distribution. If it is not the case, it can be used as a first approximation for the distance estimation error. The waveform used for the ranging test is a m-sequence of length 1023. The sequence is BPSK modulated and filtered using an SRRC pulse shaping filter with a roll-off factor of 1. The 3 dB bandwidth is

TABLE II
BEAM DEPENDENT SNR ESTIMATION

Beam index	2	4	5	6	7	8	10
SNR (dB)	-2.7	9.0	7.4	15.9	14.1	5.5	-0.2



(a) Anechoic chamber



(b) Office environment

Fig. 8. Measurement environments.

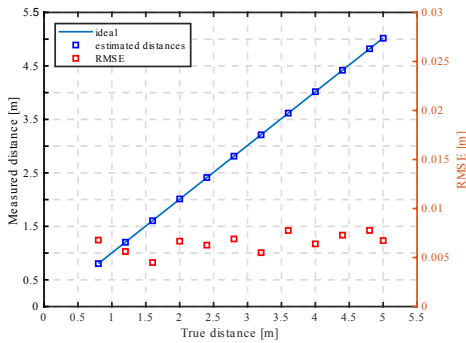


Fig. 9. Estimated distance vs true distance and root mean squared error.

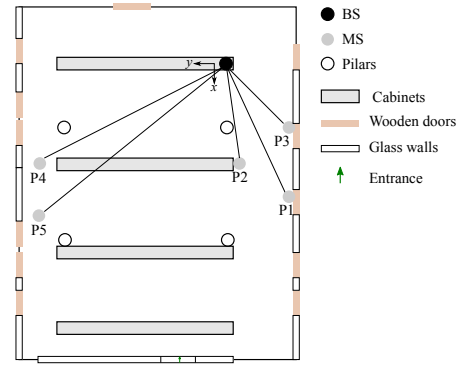


Fig. 10. The office floor plan.

1 GHz. The distance between the transmitter and the receiver is varied from 1 to 5 meters with a step of 0.4 meters. For each distance a few hundred ranging waveforms are received at the receiver and acquired using the oscilloscope. The acquired samples are processed offline. The estimated distance as a function of the true distance is shown in Fig. 9. It can be noticed that the estimated distance accurately matches the true distance. The root mean squared error (RMSE) is below 1 cm. Cumulative density function (CDF) of the distance estimates around the mean value reveals that the achievable precision falls below 2 centimeters for each of the distance measures.

B. Measurement in an office environment

In addition to the antenna chamber, the same measurements were performed in an office environment shown in Fig. 8b. The BS is placed on a wooden cabinet at the height of 175 cm, while the MS was positioned at five different locations at the height of 100 cm such that Line-of-Sight (LoS) path with the BS exists. The office floor plan with the measurement locations is illustrated in Fig. 10. In this case the measurements were performed at the frequency of 5.8 GHz in order to avoid interference from the WiFi APs used for Internet access operating in the 2.4 GHz frequency band.

For each measuring location (P1-P5), the mean estimated AoA and the mean range estimate R are reported in Table III. The estimated distance is very close to the true distance.

TABLE III
OFFICE: AO A ESTIMATION AND RANGING ACCURACY

Location	AoA ($^{\circ}$)		R (m)		Abs. error	
	True	Est.	True	Est.	AoA ($^{\circ}$)	R (cm)
P1	-26	-29.7	6.66	6.5	3.7	16
P2	-10	-15	4.45	4.47	5	2
P3	-38	-43.2	4.03	4.04	5.2	1
P4	44	44.3	6.00	6.1	0.3	10
P5	30	25	8.98	9.02	5	4

Minimal RMSE is 2.5 cm and maximal is 17 cm. Regarding the AoA maximal absolute error is around 5 degrees. The reason for the higher errors compared to the antenna chamber might be due to harsh propagation environment such as the office environment. In addition, more precise calibration of the antenna array across angles and versus temperature is needed (i.e. periodic calibration is needed).

V. CONCLUSION

In this paper, we have proposed a solution for a device localization in the mmWave band. Our solution leverages from

angular information extracted from Sub-6 communication, which is necessary to simplify the beam training process at mmWave frequencies and favors the mmWave ranging procedure. Based on the acquired angle, beam training and the ranging between a base station and a mobile station is performed. For the key parts of the described system, measurements were conducted in an anechoic chamber and an office environment. The results obtained in the anechoic chamber have shown the feasibility of the proposed method by successfully obtaining the AoA with the error less than two degrees and a centimeter precision distance estimate. In an office environment, the realistic nature of the environment, e.g. the existence of reflections, make the obtained results slightly worse than those from the anechoic chamber. Maximal angular and distance errors were five degrees and 16 cm. Nevertheless, the proposed solution can estimate fairly accurate position of an mobile node which can be made more accurate with additional calibration of the system.

Future work will include developing a more automated solution using SDR platforms supporting both Sub-6 and mmWave two-way ranging, and testing its functionality in diverse environments (indoors and outdoors) and under MS mobility.

ACKNOWLEDGMENT

This work has received funding from the European Unions Horizon 2020 research and innovation programme under grant agreement No. 671551 (5G-XHaul project). The European Union and its agencies are not liable or otherwise responsible for the contents of this document; its content reflects the view of its authors only.

REFERENCES

- [1] J. G. Andrews et al., "What Will 5G Be?", *IEEE Journal on Selected Areas in Communications*, vol. 32, no. 6, pp. 1065-1082, June 2014
- [2] W. Roh et al., "Millimeter-wave beamforming as an enabling technology for 5G cellular communications: theoretical feasibility and prototype results," *IEEE Commun. Mag.*, vol. 52, no. 2, pp. 106-113, 2014
- [3] T. S. Rappaport et al., "Millimeter wave mobile communications for 5G cellular: It will work!", *IEEE Access*, vol. 1, pp. 335-349, 2013
- [4] T. Rappaport, R. W. Heath Jr., T. Daniels, and J. Murdock, *Millimeter wave wireless communications*, Prentice Hall, 2014
- [5] IEEE Standard 802.11ad, "Wireless LAN Medium Access Control (MAC) and Physical Layer (PHY) Specifications. Amendment 3: Enhancements for Very High Throughput in the 60 GHz Band", 2012
- [6] T. Baykas et al., "IEEE 802.15.3c: the first IEEE wireless standard for data rates over 1 Gb/s," in *IEEE Communications Magazine*, vol. 49, no. 7, pp. 114-121, July 2011
- [7] J. G. Teran et al., "5G-XHaul: a converged optical and wireless solution for 5G transport networks", *Transactions on Emerging Telecommunications Technologies*, Wiley-Blackwell, 2016, doi:10.1002/ett.3063
- [8] M. Ehrig, M. Petri, V. Sark, J. G. Teran and E. Grass, "Combined high-resolution ranging and high data rate wireless communication system in the 60 GHz band", *11th Workshop on Positioning, Navigation and Communication (WPNC)*, pp. 16, 2014
- [9] M. Ehrig et al., "Reliable wireless communication and positioning enabling mobile control and safety applications in industrial environments", *IEEE International Conference on Industrial Technology (ICIT)*, Toronto, pp. 13011306, 2017
- [10] K. Witrals et al., "High-accuracy localization for assisted living: 5G systems will turn multipath channels from foe to friend", *IEEE Signal Processing Magazine*, vol. 33, no. 2, pp. 5970, 2016
- [11] F. Lemic et al., "Localization as a feature of mmWave communication", *International Wireless Communications and Mobile Computing Conference (IWCMC)*, Paphos, pp. 10331038, 2016
- [12] H. El-Sayed, G. Athanasiou and C. Fischione, "Evaluation of localization methods in millimeter-wave wireless systems", *IEEE 19th International Workshop on Computer Aided Modeling and Design of Communication Links and Networks (CAMAD)*, Athens, pp. 345349, 2014
- [13] T. Wei et al., "mTrack: high-precision passive tracking using millimeter wave radios," in *Mobile Computing and Networking*, ACM, pp. 117-129, 2015
- [14] J. Palacios, P. Casari and J. Widmer, "JADE: Zero-knowledge device localization and environment mapping for millimeter wave systems," *IEEE INFOCOM 2017 - IEEE Conference on Computer Communications*, Atlanta, GA, 2017, pp. 1-9.
- [15] F. Guidi, A. Guerra and D. Dardari, "Millimeter-wave massive arrays for indoor SLAM," *2014 IEEE International Conference on Communications Workshops (ICC)*, Sydney, pp. 114120, 2014
- [16] A. Olivier et al., "Lightweight indoor localization for 60-GHz millimeter wave systems", *IEEE International Conference on Sensing, Communication and Networking (SECON 2016)*, pp. 2730, London, 2016
- [17] A. Shahmansoori et al., "5G position and orientation estimation through millimeter wave MIMO", *IEEE Globecom Workshops*, 2015
- [18] A. Guerra, F. Guidi and D. Dardari, "On the impact of beamforming strategy on mm-Wave localization performance limits", *IEEE ICC Workshop on Advances in Network Localization and Navigation (ANLN)*, Paris, pp.809814, 2017
- [19] -, Deliverable 4.1, "Preliminary radio interface concepts for mm-wave mobile communications", mmMagic project
- [20] A. Ali, N. Gonzalez-Prelcic and R. W. Heath, "Estimating millimeter wave channels using out-of-band measurements," *2016 Information Theory and Applications Workshop (ITA)*, La Jolla, CA, 2016, pp. 1-6.
- [21] T. Nitsche, A. B. Flores, E. W. Knightly and J. Widmer, "Steering with eyes closed: Mm-Wave beam steering without in-band measurement," *2015 IEEE Conference on Computer Communications (INFOCOM)*, Kowloon, pp. 24162424, 2015
- [22] A. Patra, L. Simi and M. Petrova, "Design and experimental evaluation of a 2.4 GHz-AoA-enhanced beamsteering algorithm for IEEE 802.11ad mm-wave WLANs," *2017 IEEE 18th International Symposium on A World of Wireless, Mobile and Multimedia Networks (WoWMoM)*, Macau, 2017, pp. 1-10.
- [23] R. O. Schmidt, "Multiple Emitter Location and Signal Parameter Estimation", *IEEE Transactions on Antennas and Propagation*, Vol. AP-34, No. 3, pp. 276-280, 1986
- [24] A. J. Barabell, "Improving the resolution performance of eigenstructure based direction-finding algorithms", in *Proc. ICASSP*, Boston, MA, pp. 336339, April 1983,
- [25] R. Roy, A. Paulraj and T. Kailath, "Estimation of Signal Parameters via Rotational Invariance Techniques - ESPRIT", *Military Communications Conference - Communications-Computers: Teamed for the 90s (MILCOM)*, Monterey, pp.41.6.141.6.5, 1986
- [26] H. L. Van Trees, *Optimum Array Processing - Part IV: Detection, Estimation, and Modulation Theory*, Wiley, 2002
- [27] A. Malignaggi, M. Ko, M. Elkhoully, and D. Kissinger, "A scalable 8-channel bidirectional V-band beamformer in 130nm SiGe:C BiCMOS technology," in *IEEE MTT-S Int. Microw. Symp. Dig.*, Honolulu, HI, Jun. 2017, pp. 1-4.
- [28] www.ihp-microelectronics.com/de/forschung/drahtlose-systeme-und-anwendungen/abgeschlossene-projekte/prelocate.html
- [29] -, "Phase synchronization capability of TwinRX boards and DoA estimation", *Whitepaper*, Available at: www://kb.ettus.com